Supplemental Document

Optics Letters

# Fiber optofluidic Coriolis flowmeter based on a dual-antiresonant reflecting optical waveguide: supplement

ZHIPEI LI,[1,2] RAN GAO,[1,2,3,5] XIANGJUN XIN,[1,2,3] HAN ZHANG,[2,4,6] HUAN CHANG,[1,2] DONG GUO,[1,2] FU WANG,[1] SITONG ZHOU,[1] CHAO YU,[1] AND XINYU LIU[1]

[1]*School of Information and Electronics, Beijing Institute of Technology, Beijing 100081, China*
[2]*Key Laboratory of Photonic Information Technology, Ministry of Industry and Information Technology, Beijing Institute of Technology, Beijing, China*
[3]*Yangtze Delta Region Academy of Beijing Institute of Technology, Jiaxing 314019, China*
[4]*Key Laboratory of Noise and Vibration, Institute of Acoustics, Chinese Academy of Sciences, Beijing 100190, China*
[5]*e-mail: 6120190142@bit.edu.cn*
[6]*e-mail: zhanghan@mail.ioa.ac.cn*



Supplement DOI: https://doi.org/10.6084/m9.figshare.20018006

Parent Article DOI: https://doi.org/10.1364/OL.461516

# Fiber optofluidic Coriolis flowmeter based on dual-antiresonant reflecting optical waveguide


**Zhipei Li[1,4] , Ran Gao[1,2*,4], Xiangjun Xin[1,2,4] , Han Zhang[3,4,5], Huan Chang[1,4], Dong Guo[1,4], Fu Wang[1], Sitong Zhou[1], Chao Yu[1], and Xinyu Liu[1]**

[1]*School of Information and Electronics, Beijing Institute of Technology, Beijing, 100081, China*

[2]*Yangtze Delta Region Academy of Beijing Institute of Technology, Jiaxing, 314019, China*

[3]*Key Laboratory of Noise and Vibration, Institute of Acoustics, Chinese Academy of Sciences, Beijing, 100190, China*

[4]*Key Laboratory of Photonic Information Technology, Ministry of Industry and Information Technology, Beijing Institute of Technology, Beijing, China.*

[5]*zhanghan@mail.ioa.ac.cn*

**Corresponding author: 6120190142@bit.edu.cn*


The cross section of the HCF exposed to the $CO_2$ laser is shown in Fig. S1(a). The morphology of the HCF is almost same as the original HCF. Therefore, the scanning process did not cause the physical deformation or damage on the HCF. The normalized refractive index profile of the HCF after the scanning of the $CO_2$ laser is shown in Fig. S1(b). The refractive index modulated region can not cover the entire silica cladding. The refractive index of the upper cladding is greater than that of the below cladding because the upper cladding is directly exposed to the $CO_2$ beam. However, the double-layered Fabry-Perot etalon is only formed with the liquid and the silica cladding that is on the top of the microfluidic channel. Hence although the magnitude of the refractive index modulation is not same across different depth ranges of the HCF, the refractive index of the silica cladding on the top of the microfluidic channel is relatively uniform.

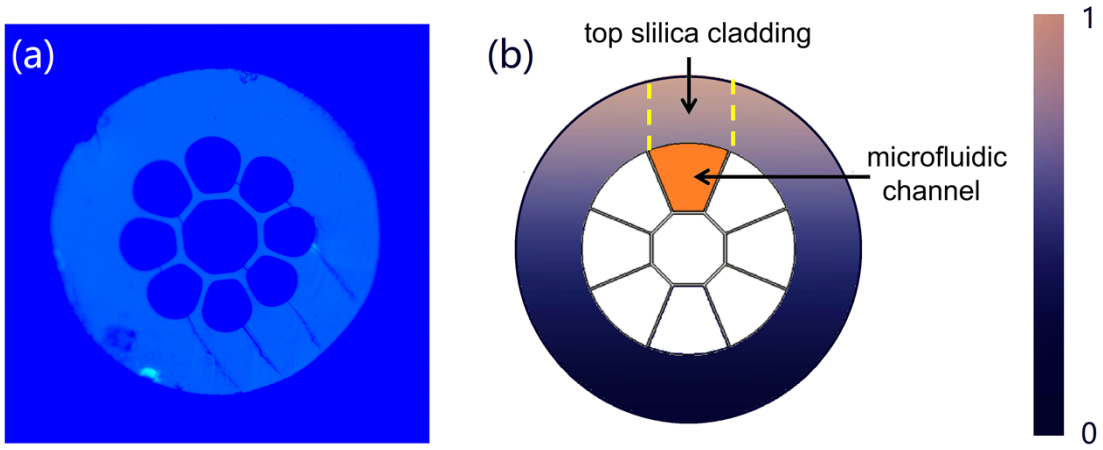

Fig. S1 (a) Cross section of the HCFexposed to the $CO_2$ laser; (b) normalized refractive index profile of the HCF after the scanning of the $CO_2$ laser .

The proposed fiber optofluidic Coriolis flowmeter is based on the ARROW effect. Hence the refractive index of the liquid is a key factor. In general, the refractive index of the liquid should be smaller than that of the silica cladding. When the refractive index of the liquid is larger than that of the silica cladding, multiple Fabry-Perot etalons (the individual liquid or silica cladding) may be formed in the HCF because the guided light can be reflected strongly on the interface between the liquid and silica cladding. As a result, too many lossy dips corresponding to different resonance condition are generated in the transmission spectrum simultaneously, which is very difficult to separate. In this experiment, the flow rate of the glycerol solution with the concentration of 70% was also tested. The refractive index of the glycerol solution with the concentration of 70% is 1.442, which is very closed to that of the silica. The transmission spectrum is shown in Fig. S2(a). The wavelength of two lossy dips are shifted to 1538.1 and 1546.8nm due to the changed resonant condition. Hence the wavelengths of the two tuneable lasers were adjusted to 1540.1 and 1547.8 nm in order to set the lasing wavelength to the slopes of the resonance dips corresponding to the two ARROWs, respectively. The relationship between the flow rate and the phase difference of the glycerol solution is shown in Fig. S2(b). The flow rate sensitivity of 11.53 deg/(μl/s) can be achieved. Due to large density of the glycerol solution (glycerol: 1.261g/cm$^3$, ethanol: 0.789 g/cm$^3$), the mass of the glycerol solution in the microfluidic channel is also large, making a higher flow rate sensitivity compared with that of the ethanol solution according to Eq. 3.

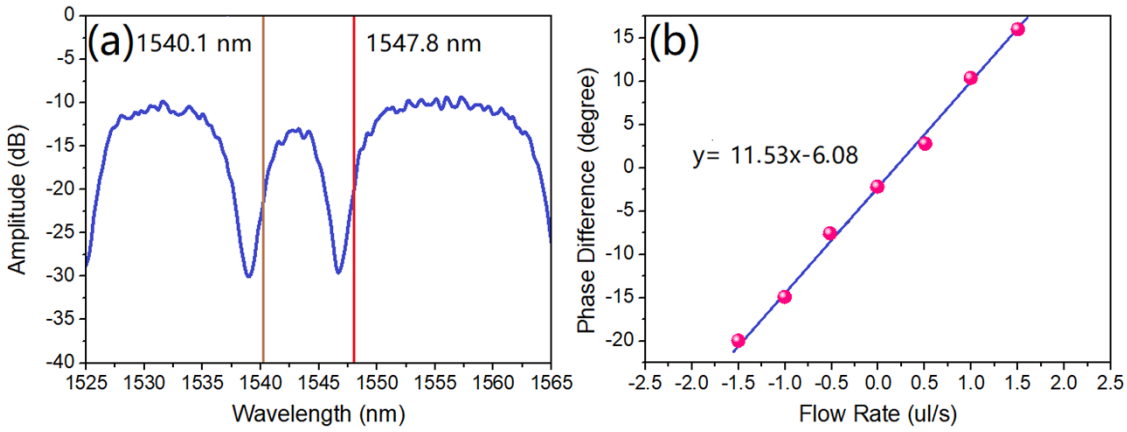


Fig. S2 (a) Transmission spectrum of the dual ARROW; (b) relationship between the flow rate and the phase difference.

The stability and time response of the Coriolis fiber optic flowmeter were also investigated. The flow rate was set to −2.0 μl/s as the initial value and was increased in 0.5 μl/s steps until a final flow rate of 2.0 μl/s was reached, and then decreased to -2.0 μl/s with the same step size. At each flow rate, the sensor was kept with 10 s. The test cycles were repeated six times, and the calculated phase difference is shown in Fig. S3(a). The sensor showed a good stability for different flow rates. Fig. S3(b) presents the standard variation for the six tests. The maximal standard variation was only 4.87% for a flow rate of −2.0 μl/s. Noted that the high flow rate make a strong Coriolis force on the HCF, resulting an unstable vibration. Hence the standard variation in high flow rate is larger than that in the low flow rate. Fig. S3(c) shows the phase difference when the flow rate was changed from −0.5 μl/s to 0 μl/s. The response time of the proposed sensor was measured as 2.48 s. The distortion in the phase difference was attributed to the unstable vibration of the ARROW induced by the changing flow rate of the ethanol.

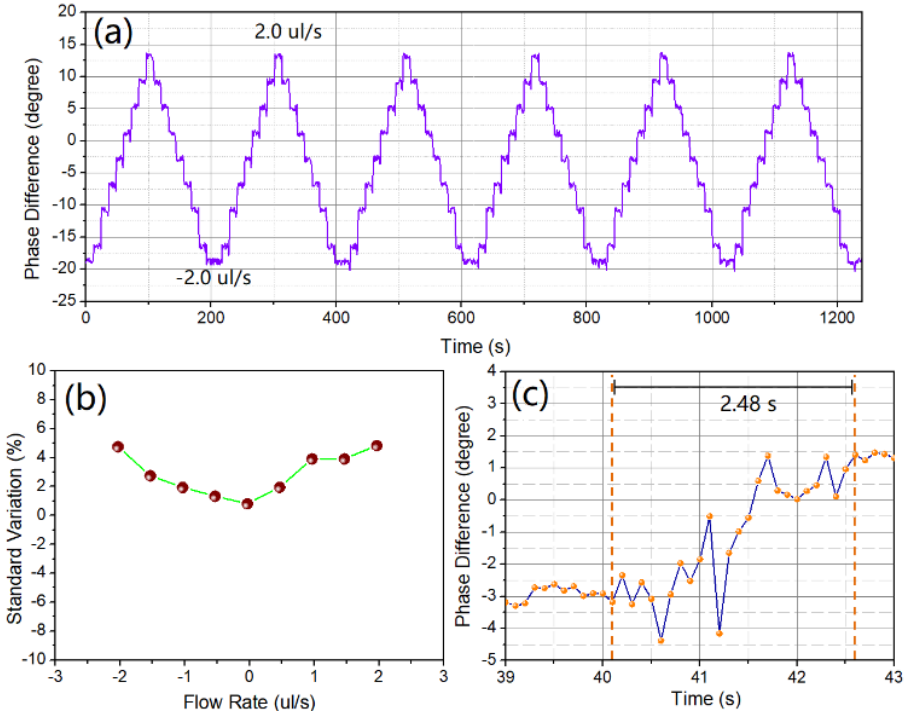


Fig. S3 (a) Phase difference at different flow rates; (b) standard variation of the phase difference for six test cycles; (c) time response.

In Fig. 4(f), there is still small deviation between the measured result and linear fit due to the structural deviation between two sides of the HCF. The structure is not uniform at every section of the HCF. Two sides of the HCF still have some small structural deviation, such as hollow hole size or silica cladding thickness, resulting in nonlinear effect for the sensor. However, the measurement bias can be compensated through the precise calibration of the sensor.